The American Journal of Human Genetics, Volume *109*

Supplemental information

A cross-species approach using an *in vivo* evaluation platform in mice demonstrates that sequence variation in human *RABEP2* modulates ischemic stroke outcomes

Han Kyu Lee, Do Hoon Kwon, David L. Aylor, and Douglas A. Marchuk

Figure S1

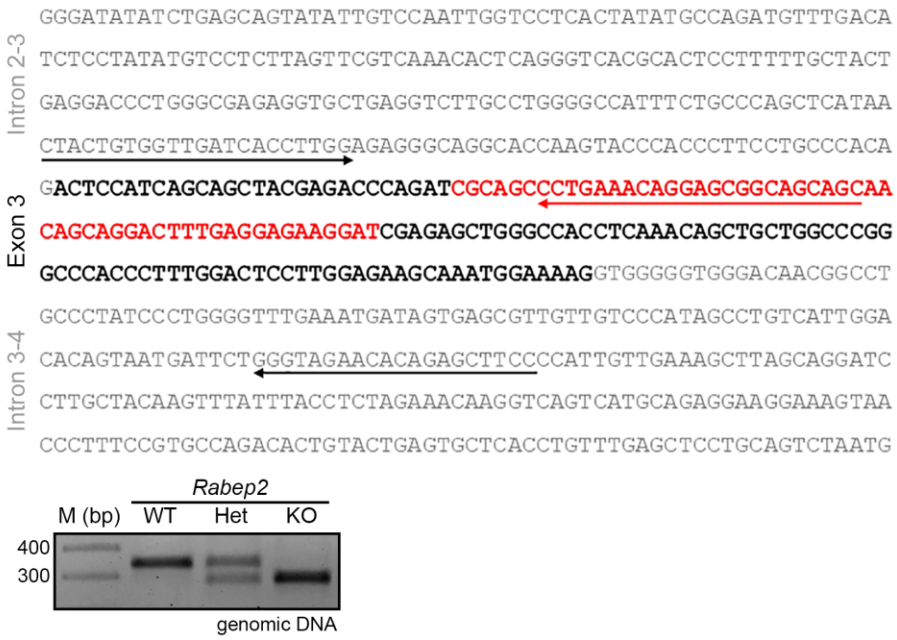

Figure S1. CRISPR/Cas9 editing creates a 55-nucleotide deletion in Exon 3 of the *Rabep2* gene. Genomic DNA sequence shows Exon 3 (in bold font) and adjacent Introns (in gray font) of *Rabep2*. A 55-nucleotide deletion indicated by red font was generated by CRISPR/Cas9 RNP using a single-guide RNA (red arrow). Forward and reverse PCR primers (black arrows) for amplification of genomic region detects a 55-nucleotide deletion in both Het and KO of *Rabep2* mice.

Figure S2

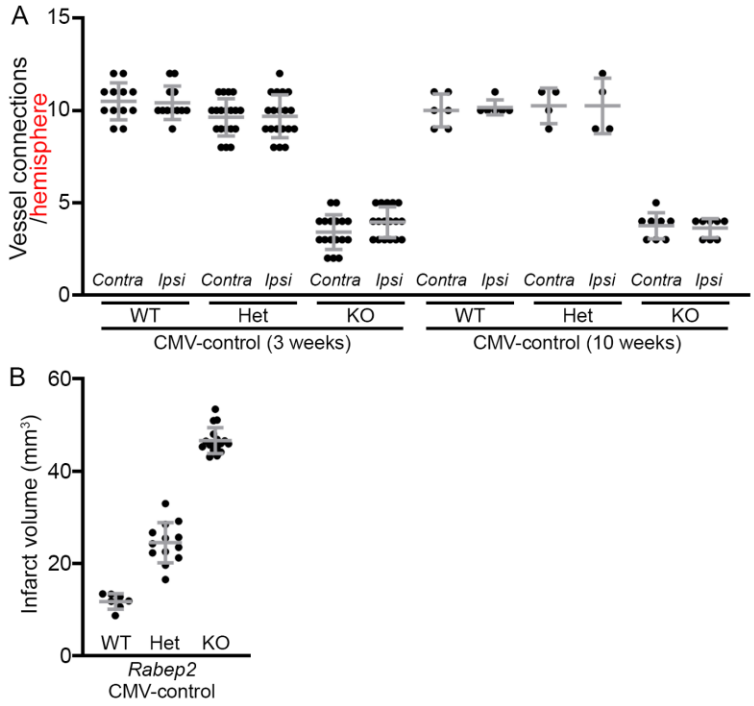

Figure S2. Phenotypes of the collateral vessel density and the infarct volume for *Rabep2* KO mice are not affected by AAV injections. (A) The scatter plots show the number of collateral vessel connections of each hemisphere, 3 and 10 weeks after AAV injections. The total number of animals for *Rabep2* WT, Het, and KO either 3 or 10 weeks after CMV-control are 12, 19, 17, 6, 7, and 8 animals, respectively. **(B)** The scatter plots present the infarct volume of each animal injected with CMV-control. The total number of animals for *Rabep2* WT, Het, and KO are 7, 13, and 17 mice, respectively.

Figure S3

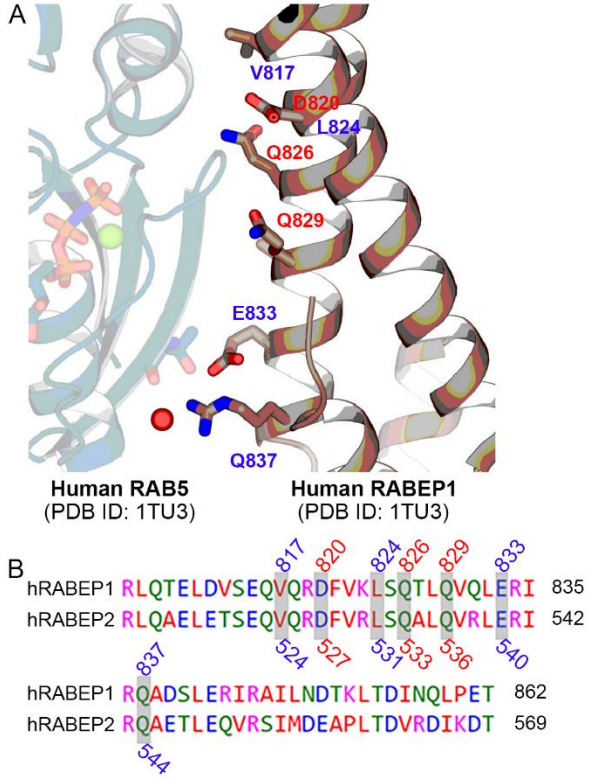

Figure S3. Interaction interface of human RABEP1 and human RAB5 complex. (A) Interaction interface between human RABEP1 and human RAB5 was previously experimentally confirmed. The interaction key residues are shown either in red (experimentally confirmed) or in blue (structurally predicted). A water molecule is shown as red sphere and a magnesium atom is shown as green sphere. **(B)** Sequence alignment between human RABEP1 and human RABEP2. Key interaction residues with RAB5 are highlighted in gray.

Figure S4

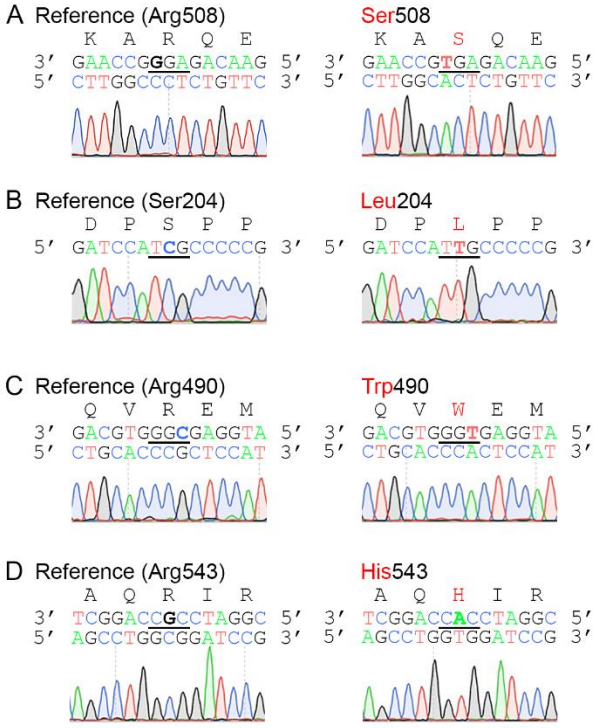

Figure S4. Sanger sequencing validation of 4 human RABEP2 coding variants. The chromatograms show the sequences of nonsynonymous coding SNP alleles between reference (WT) and coding variant in human RABEP2. **(A)** p.Arg508Ser: amino acid substituted to Ser (serine) from Arg (arginine) at amino acid position 508. **(B)** p.Ser204Leu: amino acid substituted to Leu (leucine) from Ser (serine) at amino acid position 204. **(C)** p.Arg490Trp: amino acid substituted to Trp (tryptophan) from Arg (arginine) at amino acid position 490. **(D)** p.Arg543His: amino acid substituted to His (histidine) from Arg (arginine) at amino acid position 543.

Figure S5

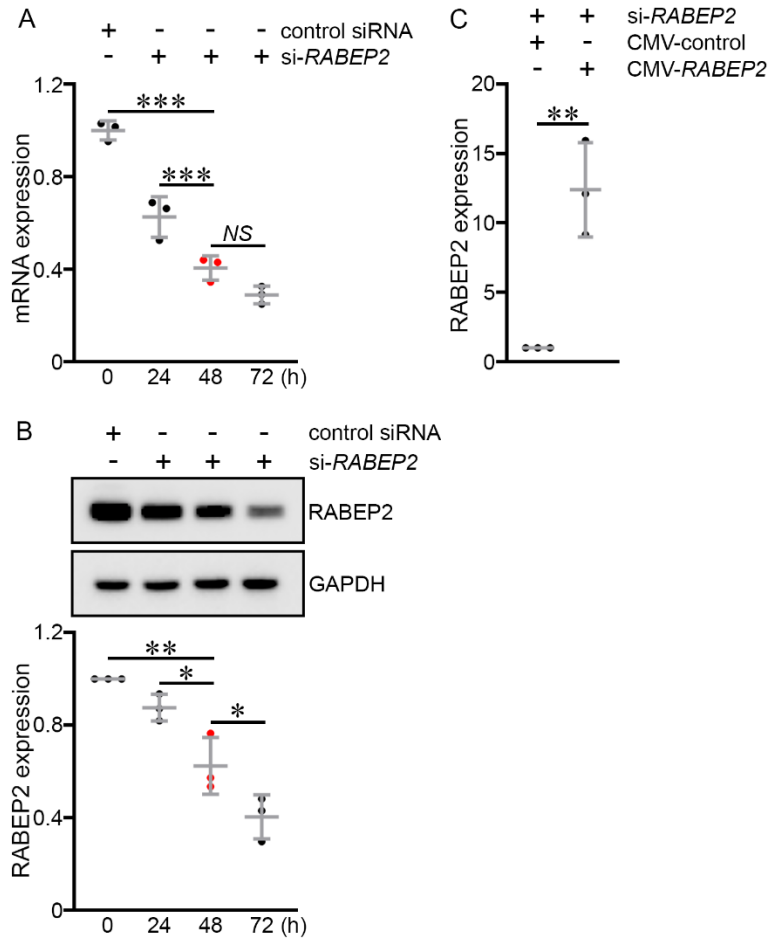

Figure S5. Efficiency of human *RABEP2* knockdown in human microvascular endothelial cells (HMECs) using siRNA. (A) Nonspecific (control) or human *RABEP2*-specific siRNA were transfected into HMECs for 72 hours. *RABEP2* mRNA levels normalized to *GAPDH* control were determined by qRT-PCR. Experiments were performed three times. Data represent the mean ± SD and statistical significance was determined by one-way ANOVA followed by Tukey's multiple comparison test (*** $p < 0.001$; *NS*, not significant). **(B)** Western blots were performed to detect RABEP2 in HMECs transfected with either control siRNA or *RABEP2*-specific siRNA. Levels of RABEP2 protein were normalized to GAPDH protein levels (control (0 h) sets to 1). Experiments

were performed three times. Data represent the mean ± SD and statistical significance was determined by one-way ANOVA followed by Tukey's multiple comparison test (∗ $p < 0.05$ and ∗∗ $p < 0.01$). **(C)** Levels of RABEP2 protein were increased by infection of CMV-*RABEP2* after knock-down of *RABEP2* for 2 days. Levels of RABEP2 protein normalized to GAPDH protein levels were determined by western blots experiments (control sets to 1). Experiments were performed three times. Data represent the mean ± SD and statistical significance was determined by two-tailed Student's *t* test (∗∗ $p < 0.01$).

Figure S6

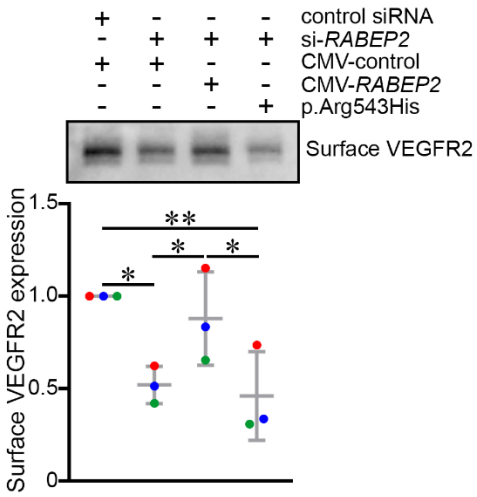

Figure S6. Wild-type human RABEP2 rescues cell surface levels of VEGFR2 but p.Arg543His RABEP2 does not. A surface biotinylation assay was performed in HMECs to measure the level of VEGFR2 on the endothelial cell membrane. After knock-down of *RABEP2*, levels of cell membrane VEGFR2 were increased to near normal levels by infection of CMV-*RABEP2* WT, but by not the p.Arg543His coding variant. Experiments were performed in triplicate with the control for each experiment (control siRNA with the CMV-control set at a value of 1). Each experimental group is then indicated by a different colored dot. Data represent the mean ± SD and statistical significance was determined by two-way ANOVA followed by Tukey's multiple comparison test (∗ $p < 0.05$ and ∗∗ $p < 0.01$).

Figure S7

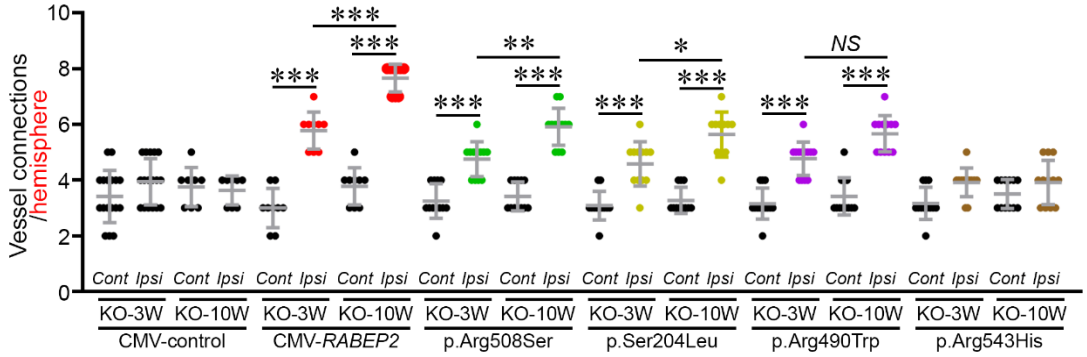

Figure S7. Human RABEP2 coding variant p.Arg543His shows no rescue of collateral vessel connections at 3 and 10 weeks after AAV injections. The scatter plots show the number of collateral vessel connections between the ACA and MCA of each hemisphere, 3 and 10 weeks after AAV injections. The total number of animals for *Rabep2* KO either 3 or 10 weeks after injections of CMV-control, *Rabep2* KO either 3 or 10 weeks after injections of CMV-*RABEP2*, *Rabep2* KO either 3 or 10 weeks after injections of CMV-*RABEP2*-p.Arg508Ser, *Rabep2* KO either 3 or 10 weeks after injections of CMV-*RABEP2*-p.Ser204Leu, *Rabep2* KO either 3 or 10 weeks after injections of CMV-*RABEP2*-p.Arg490Trp, and *Rabep2* KO either 3 or 10 weeks after injections of CMV-*RABEP2*-p.Arg543His are 17, 8, 9, 9, 12, 12, 12, 11, 13, 12, 12 and 12 animals, respectively. Data represent the mean ± SD and statistical significance was determined by one-way ANOVA followed by Tukey's multiple comparison test (∗ $p < 0.05$; ∗∗∗ $p < 0.001$; *NS*, not significant).

Tables

Chr	Position	rsID	Coding SNP	Allele			*In silico* prediction	
				count	number	frequency	SIFT	PolyPhen
16	28936427	rs115529621	p.Ala20SSer	3562	167926	0.021211724	0.16	0
	28916802	rs200118396	**p.Arg508Ser**	239	271860	0.000879129	0†	0.968†
	28922259	rs201270750	p.Thr347Ser	137	278198	0.000492455	0.27	0.145
	28922244	rs202177661	p.Val352Leu	121	278060	0.000435158	0.36	0.015
	28917045	rs201409528	p.Val491Met	111	280082	0.000396313	0.09	0.207
	28917367	rs559738470	p.Gln466Glu	107	219272	0.000487978	1	0.006
	28925840	rs769480150	**p.Ser204Leu**	91	275124	0.00033076	0.01†	0.978†
	28917045	rs201409528	p.Val491Leu	80	280082	0.000285631	0.42	0.026
	28919991	rs192852294	p.Ser395Leu	80	278986	0.000286753	0.84	0
	28916806	rs766728154	p.Gln507Leu	57	272456	0.000209208	0†	0.127
	28931252	rs199904424	p.Ser96Asn	49	272106	0.000180077	0.14	0.988†
	28931168	rs758567963	p.Arg124His	42	278940	0.00015057	0.29	0.019
	28917048	rs184144701	**p.Arg490Trp**	34	280036	0.000121413	0†	0.995†
	28922430	rs779592285	p.Arg322Gln	32	280052	0.000114264	0.33	0.36
	28925870	rs372536339	p.Thr194Met	26	275034	9.45338E-05	0.16	0.513‡
	28925859	rs764221819	p.Pro198Ser	24	244096	9.8322E-05	0.28	0.003
	28917442	rs750752217	p.Arg441Cys	21	206462	0.000101714	0†	0.993†
	28925703	rs372007568	p.Pro250Ser	21	277996	7.55407E-05	0.07	0.063
	28925904	rs550518363	p.Arg183Cys	21	273966	7.66518E-05	0.02†	0.549‡
	28925694	rs200278634	p.Arg253Cys	20	278590	7.17901E-05	0.03†	0.828‡
	28916281	rs376299848	p.Asp565Tyr	19	279334	6.80189E-05	0†	0.978†
	28926097	rs199981658	p.Glu147Gln	19	249182	7.62495E-05	0.01†	0.945†
	28916280	rs759288035	p.Asp565Val	17	279320	6.08621E-05	0†	0.93†
	28917492	rs369261936	p.Thr424Met	17	234784	7.2407E-05	0.21	0.104
	28916346	rs527458355	**p.Arg543His**	16	273404	5.85215E-05	0†	0.999†
	28922226	rs748834926	p.Arg358Trp	16	277234	5.7713E-05	0†	0.948†
	28925850	rs375415976	p.Arg201Trp	16	275346	5.81087E-05	0.03†	0.006

Table S1. *In silico*-predicted functional consequences of coding variants of human RABEP2. The list is based on human population data obtained from the Genome Aggregation Database (gnomAD) and functional effects of coding SNPs were predicted by two independent *in silico* algorithms, SIFT and PolyPhen-2. A cross (†) indicates a strong prediction of functional damage. A two-barred cross (‡) indicates possibly damaging. The four variants chosen for further study are represented in bold font.

Table S2. Raw data for all Figures. The Excel spreadsheet contains the numerical values with detailed statistical information and array information used to generate all of the figures.